MINERALOGICAL MAGAZINE

VOLUME 55 NUMBER 381 DECEMBER 1991

Vanadian allanite-(La) and vanadian allanite-(Ce) from the Hemlo gold deposit, Ontario, Canada

YUANMING PAN AND MICHAEL E. FLEET

Department of Geology, University of Western Ontario, London, Ontario N6A 5B7, Canada

Abstract

Allanite-(La) (containing up to 7.80 wt.% V_2O_3 and with La/Σ*REE* and La/Ce atomic ratios up to 0.54 and 1.45, respectively) and allanite-(Ce) (up to 8.46 wt.% V_2O_3) occur in close association with vanadian muscovite, barian tomichite and vanadian titanite in the main ore zone of the Hemlo gold deposit, Ontario, Canada. Allanite-(Ce) generally occurs as a minor constituent in cross-cutting veins or along foliation planes, whereas allanite-(La) invariably occurs in direct contact with titanite. The high V concentrations in the allanites from Hemlo are readily attributable to an adequate local source of this element, and are most likely controlled mainly by a simple substitution of V for Al in octahedral coordination. Vanadian allanite-(La) and vanadian allanite-(Ce), without any systematic differences in other constituents, are clearly distinct in *REE* composition, in respect to both the relative concentrations of La and Ce and abundances of other *REE*. The formation of both allanites (Ce- and La-rich) indicates very localised remobilisation and concentration of *REE* during a late hydrothermal alteration. The unusual *REE* composition of vanadian allanite-(La) directly reflects partitioning of *REE* with coexisting titanite, and the formation of this unusual phase may be attributable to replacement of earlier titanite with redistribution of *REE* in the solid state.

KEYWORDS: allanite-(La), allanite-(Ce), vanadian allanite, *REE* mobility, titanite.

Introduction

THE Hemlo deposit, Ontario, Canada, is anomalously enriched in vanadium and contains a large number of V-bearing minerals in the main ore zone, including vanadian muscovite, tomichite, karelianite, vanadian titanite, rutile, clinozoisite–epidote series, grossular, cafarsite, hemloite, and chromite (Harris, 1989). The present paper reports on V-bearing varieties of allanite-(La) and allanite-(Ce) from the main ore zone of the Hemlo gold deposit.

Allanite is a *REE*-rich epidote-group mineral with the general formula $A_2M_3Si_3O_{12}(OH)$ (Dollase, 1971). There are three octahedral sites $M(1)$ to $M(3)$ and two large cation sites, one of which is 9-coordinated $[A(1)]$ and the other 10-coordinated $[A(2)]$. Starting from the simple formula for clinozoisite (or zoisite), $Ca_2Al_3Si_3O_{12}(OH)$, the complex chemistry of allanite can be explained in terms of the following substitutions: Fe^{2+}, Fe^{3+}, Mg, Mn, Cr, Ti, Be, and Ge for Al in the octahedral $M(3)$ and, possibly, $M(1)$ sites, and rare-earth elements (*REE*), Y, Th, and U for Ca in the $A(2)$ site (Deer *et al.*, 1986; Treloar and Charnley, 1987; Fleischer, 1985). Minor substitution of Sr, Mn^{2+}, Na, and K for Ca in the $A(2)$ site (Exley, 1980), Ga, Be and P for Si in the

Mineralogical Magazine, December 1991, Vol. 55, pp. 497–507

tetrahedral sites (Deer *et al.*, 1986), and F^- and Cl^- for $(OH)^-$ (Deer *et al.*, 1986; Pan and Fleet, 1990*a*) may also occur in allanites. No allanite with a substantial amount of V has previously been reported.

Geological setting and Hemlo gold deposit

The Hemlo gold deposit, located approximately 35 km east of Marathon, Ontario, is situated within the east-trending, late Archean (2800–2600 Ma, Corfu and Muir, 1989*a*,*b*) Hemlo–Heron Bay greenstone belt of the Wawa subprovince of the Superior Province of North America (Muir, 1982). The geology of the Hemlo gold deposit and the Hemlo–Heron Bay greenstone belt has been described by a number of authors, e.g. Muir (1982), Macdonald (1986), Corfu and Muir (1989*a*,*b*), and Pan and Fleet (1990*b*). Most of these authors agreed that the Hemlo–Heron Bay greenstone belt has been subjected to a complex history of deposition, deformation, magmatism, metamorphism and alteration.

The main ore zone of the Hemlo gold deposit is a single orebody that contains approximately 80 mt of ore with an average grade of 7.7 g/t Au (Harris, 1989). The deposit is currently being mined as three properties: Williams mine (formerly Page–Williams mine), Golden Giant mine and David Bell mine (Teck–Corona mine), which are the three biggest gold mines in current production in Canada. The Hemlo gold deposit is unusual and perhaps unique in many aspects compared to most Archean lode gold deposits (Macdonald, 1986), and the origin of its gold mineralisation remains controversial (Macdonald, 1986; Harris, 1989).

Occurrence and petrography

Allanite has been reported as one of the least common silicate minerals in the main ore of the Hemlo gold deposit (Harris, 1989). It is observed as a minor or trace constituent in vanadium-enriched green mica schists in this study. Green mica schist is one of the important ore-bearing rock types of the Hemlo gold deposit and displays a well-developed schistosity defined by a combination of preferred orientation of green mica and an alternation of micaceous, pyritiferous and quartzofeldspathic layers. The characteristic mineral assemblage of the allanite-bearing green mica schists includes quartz, feldspar, green mica, tomichite, titanite, baryte, pyrite, molybdenite, epidote, and, locally, pumpellyite, hydrogrossular, and vesuvianite, typical of green mica schists of the Hemlo deposit (Harris, 1989). Most of the calc-silicate minerals occur in cross-cutting veins or along foliation planes, indicating a late calc-silicate alteration (cf. Pan and Fleet, 1990*a*,*b*). Harris (1989) reported that green mica from the Hemlo deposit is a 2*M* vanadian muscovite, with less than 8.5 wt.% V_2O_3. Pan and Fleet (1991) recognised that some green micas at Hemlo contain a minor amount of chromium without detectable vanadium. However, allanite does not appear to be associated with chromium-bearing green mica samples.

Allanite generally occurs as small prismatic crystals (up to 0.2 mm in maximum dimension) and displays a distinct pale green colour in plane-polarised light. Allanite is commonly found in close association with other *REE*-rich minerals, such as monazite, synchysite [(Ca(*REE*)-$(CO_3)_2F$], and apatite, in cross-cutting veins or along foliation planes, but rarely within the rock matrix. Therefore, allanite is also part of the late calc-silicate alteration. Optical and compositional zonation is not uncommon and is generally characterised by an oscillatory pattern, but sector zoning and combined oscillatory and sector zoning have also been observed (Fig. 1*a*). Individual grains of prismatic allanite are commonly altered (metamictisation), as indicated by low birefringence and low total oxide contents in electron-microprobe analyses. Allanite occurs also as very fine-grained patches or inclusions (<20 μm in maximum dimension) within or rimming other calc-silicate minerals, such as epidote (Fig. 1*b*) and vanadian titanite (Fig. 1*c*,*d*).

Mineral chemistry

The chemical composition of allanite was investigated by a JEOL JXA-8600 Superprobe electron microprobe at the University of Western Ontario following the procedures detailed by Pan and Fleet (1990*a*), with the exception that Pr was measured on the $L\alpha$ peak and corrected for La-$L\alpha$ peak-overlap using the factor of Roeder (1985). Measurements on pure metallic V standard and V-rich epidote from the study area indicate that V interference on the determination of *REE* is negligible. In this study, only unaltered (or less altered) allanite from the green mica schists of the Hemlo gold deposit are considered and representative analyses are reported in Tables 1 and 2.

As demonstrated by Pan and Fleet (1990*a*), allanite appears to form complete solid solution series with other epidote-group minerals. By definition (e.g. Levinson, 1966; Deer *et al.*, 1986), allanite requires at least 50% occupancy of the *A*(2) site by total rare-earth elements (ΣREE). Of

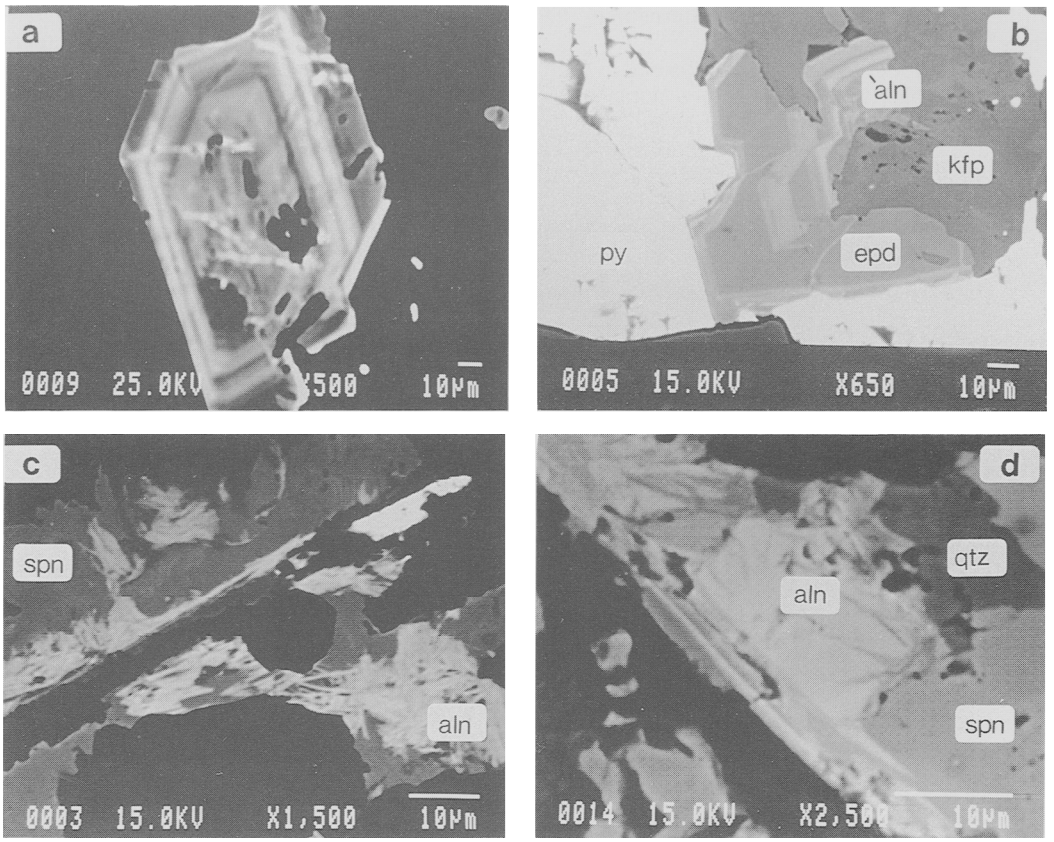

FIG. 1. Electron backscattered images showing vanadian allanites and their textural relationships with other calc-silicate minerals from the Hemlo gold deposit: (*a*) composition zonation in vanadian allanite-(Ce); (*b*) intergrowth of vanadian allanite-(Ce) with zoned vanadian epidote; (*c*) and (*d*) vanadian allanite-(La) associated with vanadian titanite (aln: allanite, epd: epidote, kpf: K-feldspar, py: pyrite, qtz: quartz, and spn: titanite).

30 spot analyses obtained by the present study, sixteen have ΣREE cations in excess of 0.5 p.f.u., the highest ΣREE cations being 0.86 (Tables 1 and 2). The remaining analyses have ΣREE cations less than 0.5 p.f.u. (Tables 1 and 2) and rigorously are *REE*-enriched epidote. However, to simplify discussion, all of the present *REE*-enriched epidote-group minerals are referred to generally as allanite(s).

The majority of the present allanite analyses have Ce as the most dominant *REE* cation (Tables 2 and 3) and, therefore, are classified as allanite-(Ce) according to the nomenclature of Levinson (1966). A notable exception is the very fine-grained allanite in direct contact with titanite (e.g. Fig. 1*c*,*d*). Here, lanthanum is the most abundant *REE*, as is clearly illustrated by La/ΣREE and La/Ce atomic ratios of up to 0.54 and 1.45, respectively (Tables 1 and 3). This type of allanite is allanite-(La) according to the nomenclature of Levinson (1966).

Fig. 2 displays a compositional gap between allanite-(Ce) and allanite-(La) in terms of *REE* composition, although considerable variation in composition does exist in both minerals. This compositional variation exists not only from grain to grain but also as pronounced zonation within individual grains. The latter, with rare exceptions, is characterised by an increase in ΣREE, accompanied by a decrease in Ca, from core to margin (Fig.1*a*). The *REE* contents of allanites, in both absolute abundances of individual elements and relative concentrations, are probably better illustrated in chondrite-normalised *REE* patterns (Fig. 3). Allanite-(La) and allanite-(Ce) from the Hemlo deposit differ from each other not only in relative concentrations of La and Ce but in other rare-earth elements as well. The

former has much steeper *REE* patterns than the latter.

Allanites from Hemlo are characterised by high V values, which range form undetectable to as much as 8.46 and 7.80 wt.% V_2O_3 (equivalent to 0.630 and 0.564 V atoms p.f.u.) in allanite-(Ce) and allanite-(La), respectively (Tables 1 and 2). Higher V values (up to 9.07 and 8.89 wt.% V_2O_3, corresponding to 0.629 and 0.636 V atoms p.f.u.) are observed also in *REE*-enriched epidote (Tables 1 and 2). The wide variation in V contents exists both from grain to grain and within individual grains. With rare exceptions, compositional zonation is characterised by an increase in V content from grain core towards grain margin (Fig. 4*a*).

The iron content of allanites from Hemlo is highly variable (Tables 1 and 2). In many cases,

Table 1. Representative compositions of allanite-(La) from the Hemlo gold deposit, weight per cent.

Analysis	1	2	3	4	5	6
SiO_2	34.38	33.62	34.20	33.99	34.30	33.52
TiO_2	0.49	0.31	0.36	0.40	0.40	0.44
Al_2O_3	13.93	16.88	16.53	17.02	17.14	18.16
Cr_2O_3	0.71	0.70	0.74	0.60	0.80	0.82
V_2O_3	8.89	8.06	7.80	7.72	7.63	6.78
FeO*	11.42	6.55	6.16	6.31	5.83	4.39
MgO	0.09	1.25	0.48	0.50	0.57	0.62
MnO	1.90	1.40	1.47	0.70	1.14	1.14
CaO	17.78	14.24	14.16	13.82	14.33	14.82
Na_2O	0.06	0.12	0.06	0.08	0.13	0.06
La_2O_3	3.88	6.74	7.82	8.77	7.99	7.48
Ce_2O_3	3.54	5.56	5.74	6.41	5.54	6.78
Pr_2O_3	0.20	0.33	0.41	0.43	0.39	0.38
Nd_2O_3	0.50	1.00	0.76	0.73	0.68	0.78
Sm_2O_3	0.10	0.21	0.19	0.15	0.16	0.21
Y_2O_3	0.11	0.14	0.16	0.12	0.11	0.17
F	nd	0.31	0.24	0.20	0.13	0.28
O=F	0.00	0.13	0.10	0.08	0.05	0.12
Total	97.05	97.30	97.07	97.91	97.22	96.55
	chemical formulae calculated on the basis of 12.5 oxygens.					
Si	3.069	3.013	3.082	3.055	3.068	3.023
Ti	0.033	0.021	0.024	0.027	0.027	0.030
Al	1.464	1.783	1.757	1.804	1.806	1.930
Cr	0.049	0.050	0.053	0.042	0.057	0.059
V	0.636	0.579	0.564	0.557	0.547	0.490
Fe^{3+}	0.455	0.105	0.000	0.000	0.000	0.000
Fe^{2+}	0.311	0.336	0.417	0.426	0.392	0.298
Mg	0.012	0.167	0.065	0.067	0.076	0.083
Mn	0.142	0.104	0.111	0.052	0.085	0.086
ΣM	3.102	3.145	2.991	2.975	2.990	2.976
Ca	1.706	1.370	1.371	1.334	1.376	1.434
Na	0.009	0.020	0.010	0.014	0.021	0.010
ΣREE	0.290	0.482	0.502	0.563	0.502	0.531
ΣA	2.005	1.872	1.883	1.911	1.899	1.975
F^-	0.000	0.086	0.064	0.054	0.035	0.075

* is the total iron content; nd is not detectable; Eu, Gd, Dy, Yb, Th, U, and Cl were also analyzed for, but were not detectable.

Table 2. Representative compositions of allanite-(Ce) from the Hemlo gold deposit, weight per cent.

Analysis	7	8	9	10	11	12
SiO_2	34.58	32.14	35.17	34.38	31.23	32.28
TiO_2	0.40	0.21	0.20	0.31	0.34	0.16
Al_2O_3	17.87	15.61	21.43	19.26	18.33	20.04
Cr_2O_3	nd	0.40	0.80	0.74	0.42	0.34
V_2O_3	9.07	8.46	6.03	1.56	0.97	nd
FeO*	5.19	8.34	3.54	9.68	9.58	8.89
MgO	0.80	0.40	0.45	0.13	0.14	0.29
MnO	0.89	1.26	1.22	1.08	1.21	1.26
CaO	16.68	11.76	18.03	16.42	10.99	11.50
Na_2O	0.16	0.17	0.08	0.05	0.14	0.15
La_2O_3	2.88	4.23	3.16	3.14	4.95	4.85
Ce_2O_3	5.65	8.76	4.81	6.13	12.18	10.39
Pr_2O_3	0.58	1.43	0.62	0.64	1.06	1.01
Nd_2O_3	1.74	3.95	1.93	2.74	4.32	4.60
Sm_2O_3	0.35	0.57	0.35	0.54	0.61	0.64
Gd_2O_3	0.26	0.28	0.25	0.23	0.52	0.52
Dy_2O_3	0.18	0.30	0.16	0.21	0.34	0.46
Y_2O_3	0.12	0.12	0.11	0.17	0.12	0.21
F	0.32	nd	nd	0.21	0.19	nd
O=F	0.13	0.00	0.00	0.09	0.08	0.00
Total	97.60	98.39	98.34	97.54	97.57	97.59
	chemical formulae calculated on the basis of 12.5 oxygens					
Si	3.036	2.987	3.000	3.081	2.986	3.008
Ti	0.026	0.015	0.013	0.021	0.025	0.011
Al	1.849	1.709	2.154	2.034	2.065	2.208
Cr	0.000	0.029	0.054	0.026	0.032	0.024
V	0.639	0.630	0.412	0.112	0.075	0.000
Fe^{3+}	0.061	0.000	0.000	0.207	0.000	0.000
Fe^{2+}	0.282	0.583	0.227	0.445	0.688	0.624
Mg	0.106	0.055	0.057	0.017	0.020	0.041
Mn	0.065	0.099	0.087	0.081	0.097	0.099
ΣM	3.028	3.107	3.004	2.943	3.002	3.006
Ca	1.572	1.173	1.651	1.579	1.128	1.155
Na	0.026	0.027	0.013	0.008	0.013	0.026
ΣREE	0.362	0.670	0.342	0.441	0.849	0.781
ΣA	1.960	1.870	2.006	2.028	1.990	1.962
F	0.080	0.000	0.000	0.057	0.054	0.000

* is the total iron content; nd is not detectable; Eu, Yb, Th, U, and Cl were also analyzed for, but were not detectable.

the total iron content can account only for the necessary Fe^{2+} for the substitution of REE^{3+} for Ca^{2+}, indicating a solid-solution series with clinozoisite (Pan and Fleet, 1990*a*). However, allanites with both Fe^{2+} and Fe^{3+} (inferred from charge-balance calculations), belonging to a solid-solution series with epidote (Deer *et al.*, 1986), are also not uncommon (Tables 1 and 2).

Other minor constituents in allanites from the Hemlo gold deposit include Ti, Cr, Mg, and Mn. The latter two, in particular, are occasionally significant in analyses with high *REE* contents (Tables 1 and 2). In addition, a minor amount of F (up to 0.3 wt.% F) has been obtained also in the vanadian allanites from Hemlo, but Cl is typically absent.

Fig.4 depicts possible mechanisms for the incorporation of V into allanites. Vandium exhibits a weak negative correlation with Al (Fig. 4*a*), indicating a simple substitution of V for Al in the octahedral sites. This correlation is improved on a plot of $\Sigma(V + Fe^{3+})$ versus Al (Fig. 4b). However, V and Fe^{3+} were probably incorporated into allanites independently, because V does not correlate with Fe^{3+}. *REE* were most likely incorporated into allanites mainly by the coupled substitution $Ca^{2+} + M^{3+} = REE^{3+} + M^{2+}$ (Fig. 4*c*; cf. Deer *et al.*, 1986; and Pan and Fleet, 1990*a*).

X-ray diffraction

A fragment of unaltered vanadian allanite-(Ce) with 7.3 wt.% V_2O_3 and 20.1 wt.% RE_2O_3 was removed from a thin-section for X-ray diffraction study using a Gandolfi camera (Cr-$K\alpha$ radiation). The calculated unit-cell parameters are a = 8.94(1), b = 5.72(2), c = 10.16(2)Å, β = 114.7(3)°, and show no significant differences from those of allanite-(Ce) (Papunen and Lindsjö, 1972). X-ray diffraction study of vanadian allanite-(La) was not possible due to its extremely-fine grain size (e.g. Fig. 1*c,d*).

Discussion

As noted above, V enrichment is a characteristic feature of parts of the Hemlo gold deposit, and a large number of V-bearing minerals, including other epidote-group minerals (clinozoisite-epidote series), have been documented in the main ore zone (Harris, 1989). Therefore, the high V contents in the allanites from Hemlo are readily attributable to an adequate local source of V and similar cation radii of V^{3+}, V^{4+}, V^{5+} and Al^{3+} in octahedral coordination (0.64, 0.58, 0.54, and 0.535Å, respectively; Shannon, 1976). It is noteworthy that the V content in the allanites from Hemlo is always similar to that in closely associated epidote, indicating that V enters equally into both allanites and epidote. This is consistent with their similar crystal structures (cf. Dollase, 1971). Burns and Strens (1967) suggested that V strongly partitions into the distorted $M(3)$ site of epidote based on polarised optical absorption spectra, and this is probably the case for V in allanites as well.

A study of 64 allanites from 51 localities by Frondel (1964) showed that Ce is always present in greater amounts than La and the La/Ce atomic ratio is generally between 0.3 and 0.5. More recently, Fleischer (1985) found that only eight of 506 allanite analyses in the literature could be considered as allanite-(La). Only one of these eight allanite-(La) analyses had a La/Ce atomic ratio substantially greater than 1.0 (1.44; Hugo, 1961), and, consequently, Fleischer (1985) concluded that the existence of allanite-(La) had yet to be confirmed.

Vanadium allanite-(La) from the Hemlo gold deposits exhibits a wide range of variation in the La/Ce atomic ratio, the highest value being 1.45

Table 3. Lanthanides and yttrium in allanites, atomic per cent (ΣRE = 100 %; data from Tables 1 and 2).

	allanite-(La)						allanite-(Ce)					
	1	2	3	4	5	6	7	8	9	10	11	12
La	46.57	48.29	51.88	52.88	53.82	47.37	24.73	21.81	28.03	22.99	20.80	21.65
Ce	42.21	39.57	37.83	38.40	37.07	42.66	48.20	44.87	42.39	44.58	50.80	46.07
Pr	2.37	2.33	2.68	2.56	2.59	2.38	4.92	7.28	5.43	4.62	4.40	4.45
Nd	5.83	6.95	4.89	4.27	4.45	4.80	14.50	19.77	16.62	19.47	17.62	19.93
Sm	1.12	1.41	1.18	0.85	1.01	1.24	2.81	2.75	2.90	3.70	2.40	2.67
Gd	nd	nd	nd	nd	nd	nd	2.01	1.30	1.99	1.51	1.96	2.09
Dy	nd	nd	nd	nd	nd	nd	1.35	1.35	1.24	1.24	1.25	1.79
Y	1.90	1.44	1.53	1.04	1.07	1.55	1.48	0.89	1.40	1.40	0.73	1.35
La/Ce	1.10	1.22	1.37	1.38	1.45	1.11	0.51	0.49	0.66	0.52	0.41	0.47
La/Nd	7.99	6.94	10.60	12.38	12.10	9.88	1.71	1.10	1.69	1.18	1.18	1.09
Σ	91.15	90.20	92.40	93.84	93.48	92.41	77.85	73.95	75.84	72.19	76.05	72.17

nd is not detectable; Σ = La + Ce + Pr.

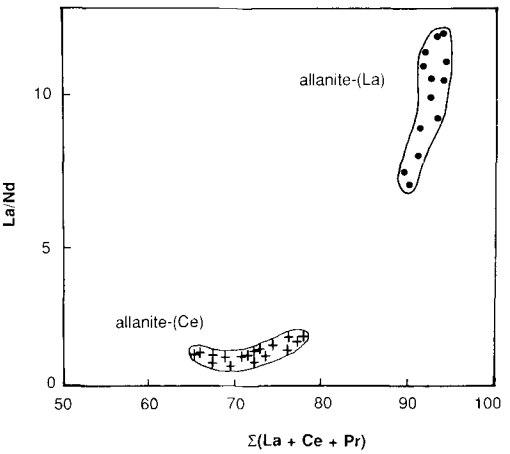

FIG. 2. La/Nd versus Σ(La + Ce + Pr) plot showing the *REE* composition of vanadian allanite-(La) (circles) and allanite-(Ce) (crosses) from the Hemlo gold deposit (after Fleischer, 1965).

and similar to that reported by Hugo (1961). Allanite-(La) from Hemlo differs from its Ce-dominant counterpart in other *REE* as well (Figs. 2,3). Furthermore, *REE*-enriched epidote with La as the dominant *REE* is also present in the Hemlo gold deposit (Table 1). Finally, there is no correlation betweeen V and La, and high V values have been obtained from both allanite-(La) and allanite-(Ce) (Tables 1 and 2). It should be emphasised, however, that allanite-(Ce) is far more common than allanite-(La) in the main ore zone of the Hemlo gold deposit.

At the White River gold occurrence, 5 km east of the Hemlo gold deposit, Pan and Fleet (1990*a*) reported an unusual halogen-bearing allanite-(Ce) and attributed its formation to a very localised remobilisation and concentration of *REE* in a late hydrothermal alteration (cf. Exley, 1980). The relative abundances of *REE* in allanite-(Ce) from Hemlo do not vary with mode of occurrence (cross-cutting veins and along foliation planes), and are similar to those in closely associated monazite and the host rock, as indicated by subparallel chondrite-normalised patterns (Fig. 5). Consistent with our previous observations, the occurrence of allanite-(Ce) in the Hemlo gold deposit most likely reflects a local

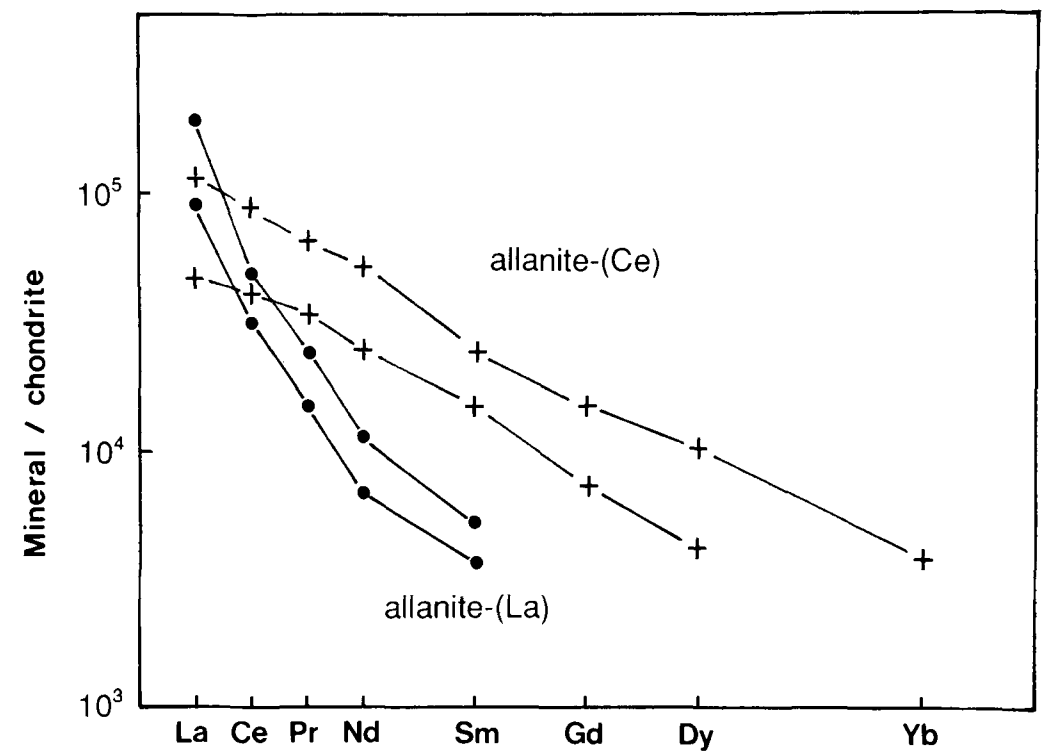

FIG. 3. Chondrite-normalised *REE* patterns of allanite-(La) and allanite-(Ce) from the Hemlo gold deposit. For symbols see Fig. 2.

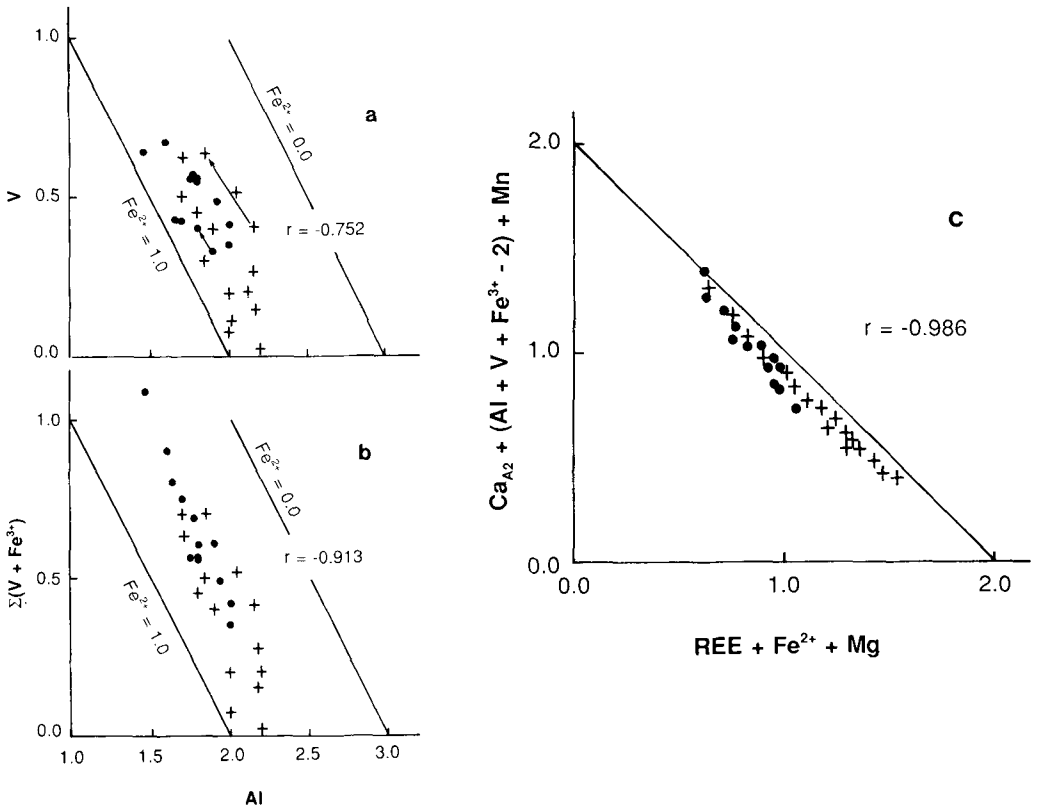

FIG. 4. Compositional variations in allanites from Hemlo: (*a*) V versus Al; (*b*) $\Sigma(V + Fe^{3+})$ versus Al; and (*c*) $Ca_{A2} + (Al + V + Fe^{3+} - 2) + Mn$ versus *REE* + Fe^{2+} + Mg. For symbols see Fig. 2; arrows indicate compositional variations from grain core to grain margin; r, correlation coefficient.

remobilisation and concentration of *REE* (cf. Exley, 1980; Pan and Fleet, 1990*a*; Fig. 5). The minor differences in *REE* composition between allanite-(Ce) and its White River counterpart (Fig. 5) are within analytical error but may reflect differences in their respective host-rock compositions.

In contrast, the distinct *REE* compositions of the allanite-(La) from Hemlo cannot be attributed to either host-rock composition or fractionation during remobilisation (cf. Murata *et al.*, 1957; Exley, 1980; Pan and Fleet, 1990*a*), because allanite-(La) coexists with allanite-(Ce) in the same rock samples on a thin-section scale. However, allanite-(La) does occur invariably in direct contact with titanite, allanite-(La) forming patches at and near the margins of titanite grains and often in intimate intergrowth relationship with it (Fig. 1*c*,*d*). An incomplete electron-microprobe *REE* composition for a large titanite grain, which hosts two allanite-(La) inclusions (patches), clearly shows a flat chondrite-normalised *REE* pattern with a positive Ce peak (Fig. 6). A simple mixing of titanite and allanite-(La) compositions in 20 to 1 proportion (the relative modal abundances of the two minerals in the titanite grain analysed) would reproduce the La/Ce ratio in both allanite-(Ce) and the whole rock (Fig. 6). It is also apparent that the calculated relative abundances of Nd and Sm are in reasonable agreement with those in allanite-(Ce) and the whole-rock as well. Fig. 6 clearly demonstrates that the whole-rock *REE* contents do partition between titanite and allanite-(La) when the two phases are in direct contact.

There are a number of studies on the distribution *REE* in titanite (Fleischer, 1978; Henderson, 1980; Exley, 1980). Fleischer (1978) found that the relative concentrations of *REE* in titanite from igneous rocks correlate with host rock

petrography. Henderson (1980) suggested that heavy *REE* are preferentially favoured by the titanite structure in which calcium is seven-fold coordinated. He also reported chondrite-normalised *REE* patterns with a positive Ce peak for titanite, with *REE* compositions determined by instrumental neutron activation analysis (INAA).

Selective incorporation of *REE* by either reduction or oxidation is well known, with removal of Eu^{2+} by early plagioclase being perhaps the best known example (Lipin and McKay, 1989). Fryer and Edgar (1977) attributed the common negative Eu-anomally in eudialyte to the early precipitation of alkali feldspar into which Eu^{2+} is preferentially incorporated. Ce^{3+} is oxidised to Ce^{4+} under oxidising conditions at the Earth's surface (Lipin and McKay, 1989), leading to a substantial decrease in ionic radius (Shannon, 1976). This would place Ce similar to heavy *REE* in terms of ionic radius and, consequently, preferred by the titanite structure. On the other hand, the higher valence would diminish the tendency of Ce to substitute for divalent Ca. Styles and Young (1983) reported the breakdown of bastnäsite-(Ce) and the weathering of fluocerite in oxidising conditions leading to the formation of bastnäsite-(La), and attributing it to the oxidation of Ce and the formation of cerianite [$(Ce^{4+}, Th)O_2$]. A considerable variation in oxygen fugacity must have occurred during the late calc-silicate alteration in the Hemlo gold deposit, as indicated by the wide range in calculated Fe^{3+} content of epidote (cf. Liou, 1973). However, oxidation of Ce^{3+} to Ce^{4+} under hydrothermal conditions has not yet been documented. Also, if Ce were present in the 4+ oxidation state, both of the present varieties of allanite would have been impoverished in Ce and *HREE*. Alternatively, the preferential partitioning of Ce and *HREE* into titanite in the presence of allanite may not be dependent on Ce^{4+}, but on some other crystal-chemical factor. Allanite-(La) might then arise from the intimate intergrowth relationship of the contemporaneous allanite and titanite.

A further possibility is that allanite-(La) is a replacement product of titanite (cf. Fig. 1*c,d*), and that the partitioning of the *REE* between

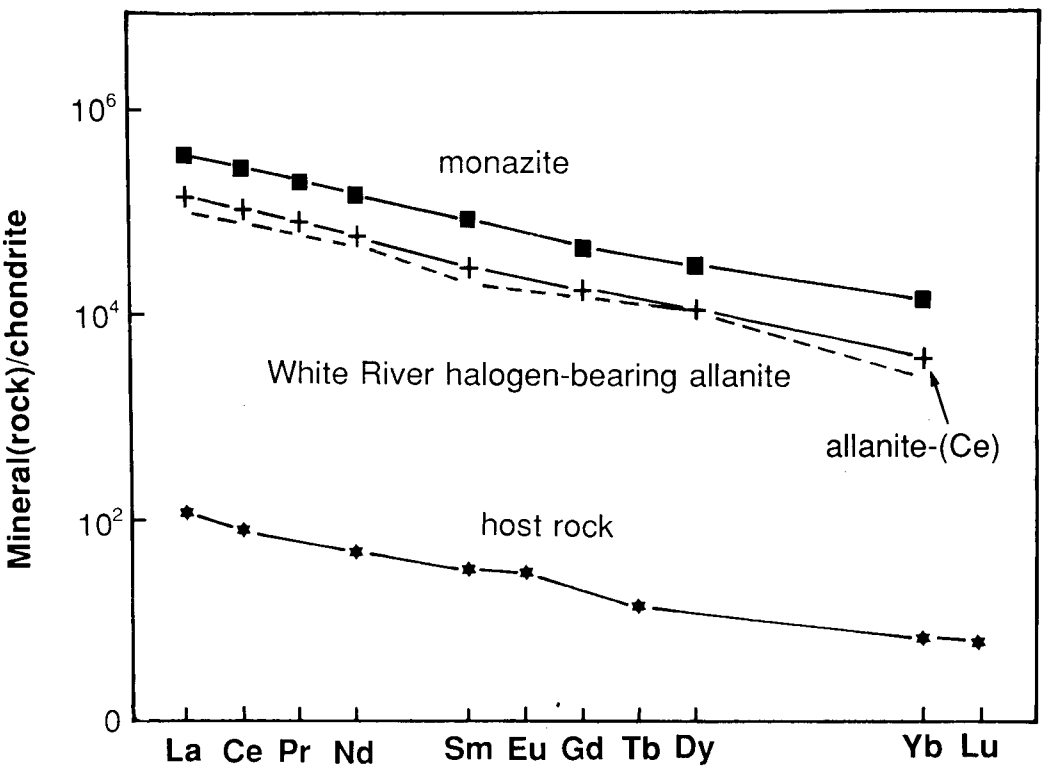

FIG. 5. Comparison of *REE* compositions in monazite (squares), allanite-(Ce) (crosses) and host rock (stars) from the Hemlo gold deposit and the halogen-bearing allanite-(Ce) (dashed line) from the White River gold occurrence (from Pan and Fleet, 1990*a*).

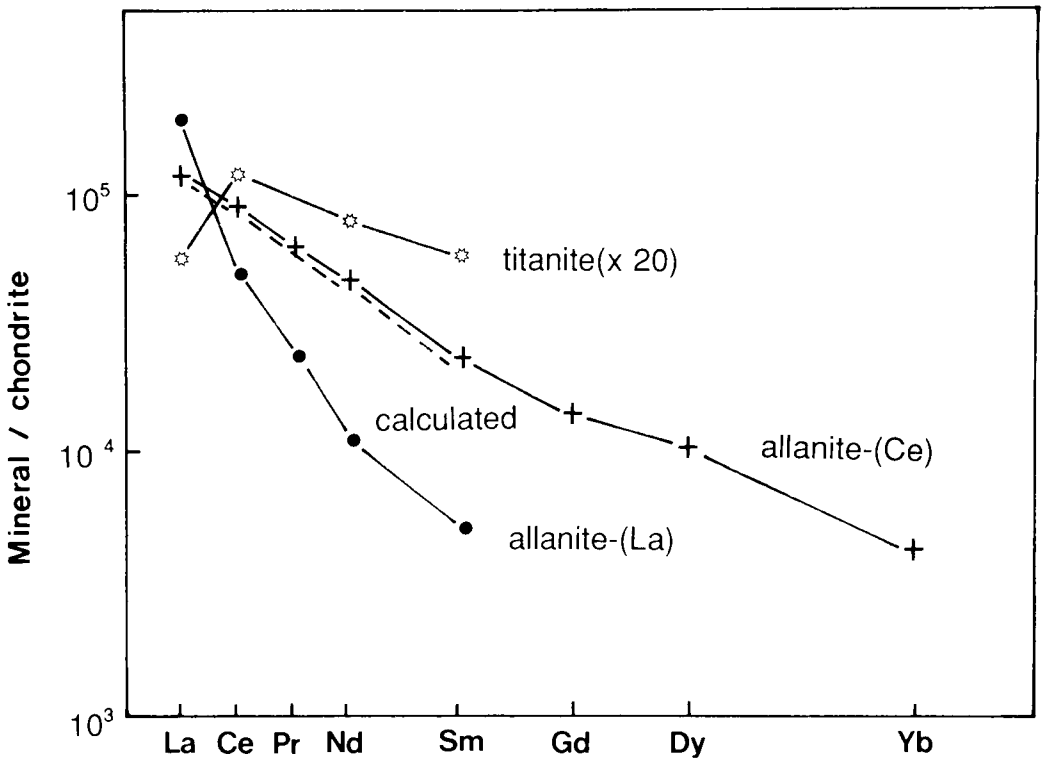

FIG. 6. Chondrite-normalised *REE* patterns of vanadian titanite (×20; open stars), allanite-(La) (circles) and allanite-(Ce) (crosses) from the Hemlo gold deposit. The fourth *REE* pattern (dashed line) is calculated from [(titanite × 20) + allanite-(La)](10/21).

allanite and titanite occurred during this replacement process. Titanite clearly replaces barian tomichite and, along with allanite-(La), appears to be part of the late calc-silicate alteration. Hence, *REE* were originally concentrated by titanite during the earlier phases of the late calc-silicate alteration. Allanite-(La), crystallising later, was intimately coupled to this local reservoir of *REE* by the replacement process. Such redistribution of *REE* during a replacement event could occur only with adequate mobility of *REE* in the titanite structure. Diffusion coefficients for *REE* in titanite are not available, but the occurrence of allanite-(La) could indeed point to significant mobility of lanthanides and actinides in titanite at relatively low temperatures. This could have profound consequences for the utility of titanite for age dating alteration events in rocks (cf. Corfu and Muir, 1989*b*).

Finally, Pan and Fleet (1990*a*) suggested that unusually high halogen contents in the White River allanite indicate elevated F and Cl contents in the hydrothermal fluid, and such a fluid could promote the mobility of *REE* and result in their local concentration (cf. Michard and Albarède, 1986; Lottermoser, 1989). In comparison with their White River counterpart, the allanites from Hemlo are not significantly enriched in halogen contents (Tables 1 and 2). However, considerable amounts of halogens are present in a large number of vein minerals (such as pumpellyite, hydrogrossular, vesuvianite, tremolite, phlogopite, apatite and synchysite) from the main ore zone of the Hemlo gold deposit (Pan and Fleet, unpubl. data). It is most likely, therefore, that the hydrothermal fluid at Hemlo also contained elevated F and Cl contents. A detailed investigation on the *P–T–X* conditions of this late hydrothermal alteration in the main ore zone of Hemlo gold deposit is currently underway.

Acknowledgements

We thank M. Fleischer and N. D. MacRae for helpful suggestions and discussion, two anonymous referees for helpful comments and G. Raade for editorial assistance. Logistic support in the field was provided by G. Skrecky of the Williams mine (Williams Operating Corporation)

and D. G. McIlveen and P. Johnson of the Golden Giant mine (Hemlo Gold Mines). One sample used in this study was collected by R. E. Goad. Technical assistance was obtained from R. L. Barnett, Y. Cheng, J. Forth, and D. M. Kingston. This work was supported by an Ontario Geological Survey Geoscience Research Grant (No. 393 to MEF).

References

Burns, R. G. and Strens, R. G. J. (1967) *Mineral. Mag.*, **36**, 204–26.

Corfu, F. and Muir, T. L. (1989*a*) *Chem. Geol.*, **79**, 183–200.

——— (1989*b*) Ibid. **79**, 201–23.

Deer, W. A., Howie, R. A., and Zussman, J. (1986) *Disilicates and ring silicates. Rock-forming minerals*, **1B**, Longmans, London.

Dollase, W. A. (1971) *Am. Mineral.*, **56**, 447–64.

Exley, R. A. (1980) *Earth Planet. Sci. Lett.*, **48**, 97–110.

Fleischer, M. (1965) *Geochim. Cosmochim. Acta*, **29**, 755–72.

—— (1978) *Am. Mineral.*, **63**, 869–73.

—— (1985) *Bull. Geol. Soc. Finland*, **57**, 151–5.

Frondel, J. W. (1964) *Am. Mineral.*, **49**, 1159–77.

Fryer, B. J. and Edgar, A. D . (1977) *Contrib. Mineral. Petrol.*, **61**, 35–48.

Harris, D. C. (1989) *Geol. Surv. Can., Econ. Geol. Rep.*, **38**, 88pp.

Henderson, P. (1980) *Contrib. Mineral. Petrol.*, **72**, 81–5.

Hugo, P. J. (1961) *Rep. S. Africa Dep. Mines, Geol. Surv. Bull.*, **37**, 1–65.

Levinson, A. A . (1966) *Am. Mineral.*, **51**, 152–8.

Liou, J. G. (1973) *J. Petrol.*, **14**, 381–413.

Lipin, B. R. and McKay, G. A . (1989) *Geochemistry and mineralogy of rare earth elements. Rev. Mineral.*, **21**, Mineral. Soc. Am., 348pp.

Lottermoser, B. G. (1989) *Mineral. Deposita*, **24**, 92–9.

Macdonald, A. J. (1986) *Proc. Gold'86, Intern. Symp. Geol. Gold* (Toronto, 1986), 517pp.

Michard, A. and Albarède, F. (1986) *Chem. Geol.*, **55**, 51–60.

Muir, T. L. (1982) *Ont. Geol. Surv. Rep.*, **217**, 65pp.

Murata, K. J., Rose, H. J., Jr, Carron, M. K., and Glass, J. J. (1957) *Geochim. Cosmochim. Acta*, **11**, 141–61.

Pan, Y. and Fleet, M. E. (1990*a*) *Can. Mineral.*, **28**, 67–75.

——— (1990*b*) *Ont. Geol. Surv. Misc. Pap.*, **150**, 13–26.

——— (1991) *Can. Mineral.*, **29** (in press).

Papunen, H. and Lindsjö, O. (1972) *Geol. Soc. Finland Bull.*, **44**, 123–9.

Roeder, P. L. (1985) *Can. Mineral.*, **23**, 263–71.

Shannon, R. D. (1976) *Acta Cryst.*, **A32**, 751–7.

Styles, N. T. and Young, B. R. (1983) *Mineral. Mag.*, **47**, 41–6.

Treloar, P. J. and Charnley, N. R. (1987) *Can. Mineral.*, **25**, 413–8.

[*Manuscript received 28 November 1990; revised 20 February 1991*]